Journal of Forestry Research (2025) 36:62
https://doi.org/10.1007/s11676-025-01856-5

ORIGINAL PAPER

A hybrid method for tree-level forest planning

Yusen Sun[1,2] · Xingji Jin[1] · Timo Pukkala[1,3] · Fengri Li[1]

Received: 22 January 2025 / Accepted: 18 March 2025 / Published online: 5 May 2025
© The Author(s) 2025

Abstract Forest inventory is increasingly producing information on the locations and sizes of individual trees. This information can be acquired by airborne or terrestrial laser scanning or analyzing photogrammetric data. However, all trees are seldom detected, especially in young, dense, or multi-layered stands. On the other hand, the complete size distributions of trees can be predicted with various methods, for instance, kNN data imputation in an area-based LiDAR inventory, predicting the parameters of a distribution function from remote sensing data, field sampling, or using histogram matching and calibration methods. The predicted distribution can be used to estimate the number and sizes of the non-detected trees. The study's objective was to develop a method for forest planning that efficiently uses the available tree-level data in management optimization. The study developed a two-stage hierarchical method for tree-level management optimization for cases where only part of the trees is detected or measured individually. Cutting years and harvest rate curves for the non-detected trees are optimized at the higher level, and the cutting events of the detected trees are optimized at the lower level. The study used differential evolution at the higher level and simulated annealing at the lower level. The method was tested and demonstrated in even-aged *Larix olgensis* plantations in the Heilongjiang province of China. The optimizations showed that optimizing the harvest decisions at the tree level improves the profitability of management compared to optimizations in which only the dependence of thinning intensity on tree diameter is optimized. The approach demonstrated in this study provides feasible options for tree-level forest planning based on LiDAR inventories. The method is immediately applicable to forestry practice, especially in plantations.

Keywords Forest planning · Simulated annealing · Unmanned aerial vehicle (UAV) · Laser scanning · *Larix olgensis* · Management optimization

Project funding: This research was supported by the Natural Science Foundation of China (U21A20244 and 32071758).

The online version is available at https://link.springer.com/.

Corresponding editor: Lei Yu

✉ Xingji Jin
xingjijin@nefu.edu.cn

✉ Timo Pukkala
timo.pukkala@uef.fi

[1] Key Laboratory of Sustainable Forest Ecosystem Management-Ministry of Education, School of Forestry, Northeast Forestry University, Harbin 150040, People's Republic of China

[2] School of Environmental and Resources Science Conservation, Zhejiang A&F University, Hangzhou 311300, People's Republic of China

[3] University of Eastern Finland, P.O. Box 111, 80101 Joensuu, Finland

Introduction

Forest ecosystems play an essential role in the global carbon cycle, provide wood and amenities, maintain biodiversity, and protect soil against erosion (e.g., Baskent 2020; Kappen et al. 2020). Forest inventories are the basis of forest management, which is important for the sustainability of the different functions of forests (Pan et al. 2011; Leite et al. 2020).

One of the inventory methods is light detection and ranging (LiDAR). It can capture detailed information on forest canopies in three dimensions over large areas (Gobakken and Næsset 2004). Forest inventories employing

airborne laser scanning (ALS) data have become a common topic in forest research (Quan et al. 2021; Sun et al. 2021). The ALS-based forest inventory methods are often divided into two groups: individual tree detection (ITD) and area-based approach (ABA) (Næsset 2002).

In the ABA approach, metrics calculated from ALS data can be used to impute field-measured data for the spatial units for which the ALS statistics are calculated (Packalén et al. 2012). These units may be raster cells, nano segments, segments, or stand compartments (Packalén and Maltamo 2008; Pippuri et al. 2013). If diameter distributions have been measured in the field plots, they can be imputed to the calculation units (Maltamo et al. 2006; Yu et al. 2010; Packalén et al. 2012; Hao et al. 2022).

In the ITD approach, individual trees are delineated, and the approximate spatial locations of the segmented trees are determined by using the canopy height model (Hao et al. 2021; Sun et al. 2022a). The drawback of ITD inventories is that all trees are seldom detected (Vauhkonen et al. 2012). There may be omission errors (false negatives), which are trees that are not detected from remote sensing data (Jeronimo et al. 2018). The other type of error is commission errors (false positives), which are the field-measured trees that cannot be matched with the segmented trees. In the ITD literature, the number of detected trees divided by the true number of trees is called "recall" (Zaforemska et al. 2019).

Zaforemska et al. (2019) compared the performance of five segmentation algorithms in ITD. Their analyses suggest that the continuously adaptive mean shift method (Xiao et al. 2016) was the best. The detection rate (recall) varied from 0.35 to 1.0, depending on the segmentation method, stand type, and parametrization of the segmentation method. In Jeronimo et al. (2018) the proportion of detected trees increased from about 0.25 to 0.8 when the relative height of trees increased from 20 to 100%. In Sun et al. (2022a), 22% of field-measured trees were not detected from LiDAR data. In the study of Mohan et al. (2017), the detection rate (recall) ranged from 0.71 to 1.0 among the 30 analysed plots.

The ITD methods typically produce tree heights and crown areas, although most growth, survival, biomass, and volume models need the stem diameter at breast height as a predictor. Sun et al. (2022a) used unmanned aerial vehicle (UAV) for laser scanning (ULS) in even-aged larch plantations. They compared six different algorithms to predict tree diameters of larch (*Larix olgensis*) plantations using both tree-level and stand-level ULS metrics as predictors. Of the tested methods, support vector regression turned out to be the best with an RMSE of 1.98 cm (14%) in the modeling dataset and 2.22 cm in an independent validation dataset. Hao et al. (2021) used non-linear mixed-effect modeling and obtained an RMSE of 1.94 cm in the diameter prediction of *Larix olgensis* plantations.

As an alternative to predicting tree diameters, Kansanen et al. (2019) proposed a histogram matching method where the distribution of breast height diameters is obtained as a transformation of the distribution of the crown diameters of individually detected trees. This method mitigates the problem that many of the smallest trees remain undetected in ITD inventories. Hao et al. (2022) predicted the diameter distributions of trees by predicting or recovering the parameters of the Weibull function from UAV LiDAR metrics. Xu et al. (2014) used calibration to modify the ITD-derived height distributions of trees to better correspond to the empirical height distributions. Calibration helped to improve the estimation of the number of small, suppressed trees. The edge-tree correction methods described in Packalen et al. (2015) and Pascual (2019) use ITD to improve the computation of the LiDAR metrics for field plots, enhancing the accuracy of area-based methods.

Although ITD methods seldom detect all trees of the stand, they are competitive with area-based methods in estimating stand characteristics. For example, Yu et al. (2010) obtained an RMSE of 6.42% for mean height and 20.90% for volume when area-based estimation was used whereas the RMSE was 5.69% for mean height 18.55% for volume when ITD was used. In Peuhkurinen et al. (2011) an area-based statistical approach and ITD were close to each other in basal area and volume estimation, but the diameter distribution was estimated slightly better with the area-based method.

ITD offers the possibility to use tree-level data in forest planning (Contreras and Chung 2013; Wing et al. 2019; Packalen et al. 2020; Pascual 2021; Pascual and Guerra-Hernández 2022). Some of the suggested methods optimize a rule that is used to select harvested trees (Pukkala et al. 1998, 2015). The other research line is to optimize the harvest moment separately for each tree, using combinatorial optimization (e.g., Fransson et al. 2020). Optimizing the harvest year separately for every tree is technically straightforward but the approach may lead to extremely large decision spaces if several cuttings are optimized and the rotation periods are long. To mitigate the problem, Sun et al. (2022b) proposed a two-stage hierarchical problem formulation where the cutting years are optimized at the higher level and the optimal cutting event is found for each tree at the lower level. Sun et al. (2022b) used differential evolution (Storn and Price 1997) to optimize the cutting years and simulated annealing (Bettinger et al. 2002) to assign the trees optimally to different cutting events.

When management planning uses tree-level optimization methods, the non-detected trees can be "generated" based on the difference between the predicted or imputed diameter distribution of all trees and the diameter distribution of detected trees. However, it may not make sense to optimize their cutting events individually because non-detected trees cannot be identified in the forest when the thinning is done.

Most of the non-detected trees are dominated individuals sheltered by the dominant canopy. Because of this, (Sun et al. 2022a) suggest that a hybrid method should be developed where the cutting event is optimized at the tree level only for the detected trees. For the other trees, the harvest decisions of partial cuttings should use an optimized tree selection rule.

The objective of this study was to develop and demonstrate the hybrid method for tree-level planning where tree-level optimization is used for the detected trees and an optimized thinning intensity function is used for the non-detected trees. The other objective was to analyze the economic benefit of tree-level planning. The hypothesis was that the profitability of forest management improves when harvest decisions are optimized at the tree level whenever possible, compared to a case where only a thinning intensity function is optimized. The thinning intensity function gives the proportion of removed trees in different diameter classes. The study used ULS data from *Larix olgensis* plantations located in the Heilongjiang province of Northeast China.

Material and methods

Study sites and field data

The study area is in the Mengjiagang forest farm of Huanan country in Heilongjiang Province of Northeast China (45°30′16″ N–46°20′20″ N, 130°32′0″ E–130°52′6″ E) (Fig. 1). The Mengjiagang forest farm covers 15,503 ha. It has a temperate continental monsoon climate with the mean annual temperature ranging from 2.7 °C to 3.9 °C, and average annual precipitation ranging from 450 to 700 mm. Most forests are plantations dominated by coniferous tree species, predominantly *Larix olgensis*, *Pinus koraiensis*, *Pinus sylvestris*, and *Picea asperata*. The area is characterized by gentle slopes and low-elevation hills, with an average elevation of approximately 250 m a.s.l. with a range of 180–450 m (Hao et al. 2021; Sun et al. 2022c).

Larch (*Larix olgensis*) is an abundant timber tree species in northeast China with fast growth at a young age and high-quality wood. Larch plantations cover 31% (4800 ha) of the whole plantation forests in the Mengjiagang Forest Farm. The initial planting density of most larch plantation forests has been 3300 ind. ha^{-1} and a typical density of near-mature stands is around 500 ind. ha^{-1} (Sun et al. 2021).

In the present study, nine rectangular sample plots (20 m × 30 m or 30 m × 30 m) measured in even-aged larch plantations were used for the analyses (Table 1). Four plots were measured in middle-aged, 44- or 47-year-old stands. Five plots were measured in younger, 13- or 17-year-old plantations (Table 1). No commercial cuttings had been conducted in the young plots and two cuttings had been conducted using maximal thinning intensity 30 or 45% in the middle-aged plots before the measurement. The diameter at breast height (DBH) of all trees greater than 5 cm was measured using diameter tape. The total tree height was measured for all trees using a Vertex IV instrument with a height resolution of 0.1 m. The site index of the plot was calculated with the model of Dong et al. (2021).

A real-time kinetic (RTK) global navigation satellite system (GNSS) device (UniStrong G10A, Beijing, China) was used to determine the geographical coordinates of all trees of the sample plots. These field measurements were conducted shortly after the LiDAR flights.

ULS data acquisition and individual tree detection

ULS data were acquired with a RIEGL mini VUX-1UAV LiDAR scanner (www.riegl.com/products/unmanned-scanning/rieglminivux-1uav) on 12 August 2019 carried by a DJI M600 Pro eight-rotor unmanned aerial vehicle platform. The services provided by RIEGL (RIEGL Laser Measurement Systems GmbH, Horn, Austria) included rehabilitating the flight trajectory by post-processing of the GNSS and Inertial Measurement Unit (IMU) records and basic data processing using the software package RiPROCESS (http://www.riegl.com/products/software-packages/riprocess/) to generate ULS point cloud data (Brede et al. 2019). The laser scanner had a 330° field of view (FOV) and the laser pulse repetition rate was 380 kHz. The maximum echo number was 5, with an accuracy of 5 mm. The average point densities of the plots ranged from about 120 to 136 pulses/m^2. The specifications for the ULS survey are summarized in Table 2.

Before individual tree detection from the ULS point cloud data, noise points were removed from the raw LiDAR point clouds by using a Gaussian-smoothing filter (Wang et al. 2022). Then, the LiDAR points were classified as ground and non-ground points using a cloth simulation filter with 0.5 as the parameter value of grid resolution, 0.6 as the time step, and 3 as the rigidness. The average density of ground points was 17 pulses/m^2. The digital elevation model (DEM) with a 1 m spatial resolution was calculated using the ground points and Kriging interpolation (Liu et al. 2018). Finally, the height of all non-ground point clouds was height-normalized by the DEM. The normalized point clouds were clipped with the boundaries of the rectangular sample plots with a two-meter buffer zone. The canopy height model (CHM) in 0.1-m spatial resolution was constructed from the normalized point cloud using the GridSurfaceCreate function for individual tree delineation (Leite et al. 2020).

The individual tree detection (Fig. 2) was based on the watershed segmentation method of the CHM. A detailed description of the delineation algorithm is presented by Chen et al. (2006). In this study, the watershed segmentation

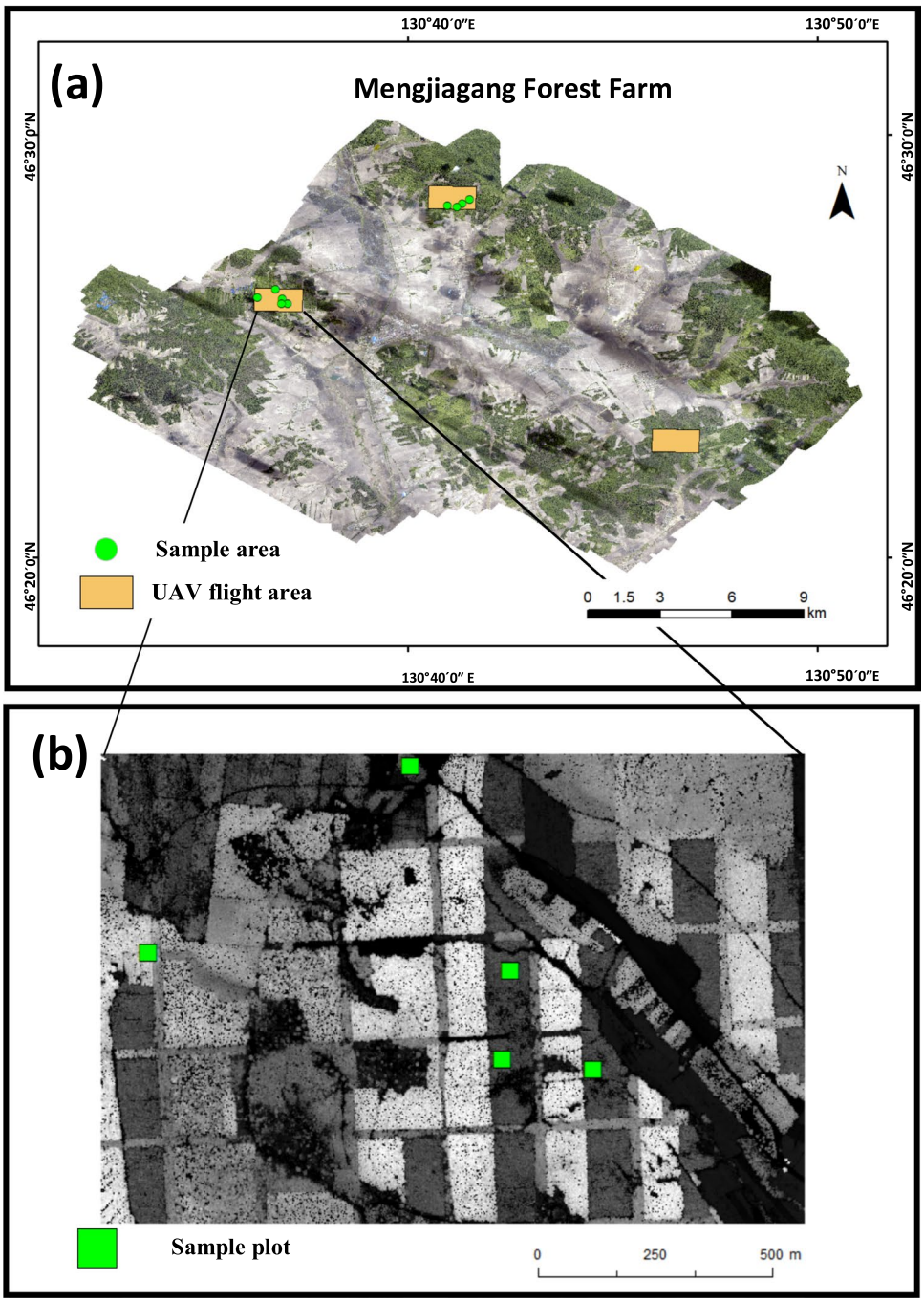

Fig. 1 a Map of the Mengjiagang forest farm in Heilongjiang province, northeast China, showing the study area location. b the CHM data and sample plots

algorithm used 90 as the buffer size and 0.8 as the crown base height threshold.

The maximum height of each polygon was taken as the treetop. The tree-to-tree matching procedure was done by evaluating the horizontal distance between field-measured and the segmented trees. Segmented trees whose treetops were encompassed within the crown radius of the reference trees were assigned as candidate matches. Subsequently, among multiple candidate trees, the one exhibiting the minimum combined difference in height and distance relative to the reference tree was selected as the optimal match. Those LiDAR-detected trees that could be matched with field-measured trees were used in subsequent analyses (Fig. 2). In total, 63% – 95% of the trees were correctly matched with field-measured trees. Field-measured trees not matched with any LiDAR-detected trees were considered omission errors (false negatives). The average detection rate (recall) was 0.69 among the nine plots that were used in the study. The average detection rate was 0.58 for

Table 1 Growing stock characteristics of the plots used in the study

Age (year)	Site index (m)	DBH* range (cm)	DBH mean (cm)	Height range (m)	Height mean (m)	Number of trees		Basal area (m^2 ha^{-1})
						per plot	per ha	
17	16.68	5.1–15.5	8.9	6.0–11.6	8.9	171	2850	19.4
17	18.00	5.0–14.3	8.5	6.8–12.9	9.9	216	3600	21.3
17	18.88	5.0–17.4	8.5	6.7–17.4	9.5	190	3167	19.3
13	24.50	5.0–14.4	7.3	4.0–16.0	8.8	206	3433	11.4
13	25.94	5.0–16.9	8.0	5.5–15.6	10.2	172	2867	17.9
44	17.48	14.6–31.0	21.6	9.7–23.1	15.9	63	677	37.3
47	18.66	15.0–31.8	21.7	9.9–25.9	19.2	68	1050	27.9
44	19.45	10.4–28.4	19.6	11.6–25.4	18.6	131	1363	23.7
44	21.17	13.2–32.8	22.0	14.9–27.5	21.3	93	1033	31.9

* Diameter at breast height

Table 2 ULS acquisition specifications

Flight speed (m s^{-1})	Flying altitude (m)	Maximum range (m)	Beam divergence (mrad)	Laser wavelength (nm)
10	180	250	0.5	1550

the young, 13–17 years old plots, and 0.73 for the older, 41–44 years old plots.

Outline of the method

The method proposed in this article used combinatorial optimization to find the optimal cutting event individually for all detected trees (Fig. 3). This study used simulated annealing (SA) to solve the combinatorial optimization problems, although several other metaheuristics could be

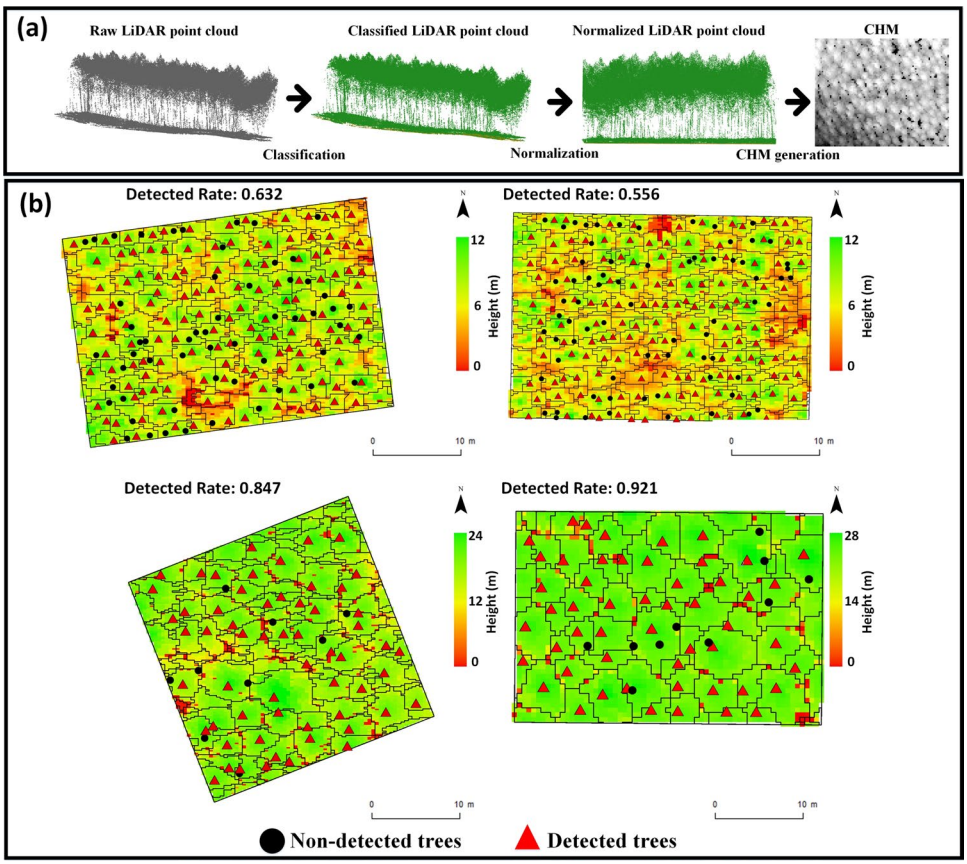

Fig. 2 The UAV data preprocessing (a) and examples of individual tree delineation (b). Polygon boundaries represent individual tree crowns. The top row of (b) shows two young plots (13–17 years) and the bottom two older (41–44 years) plots

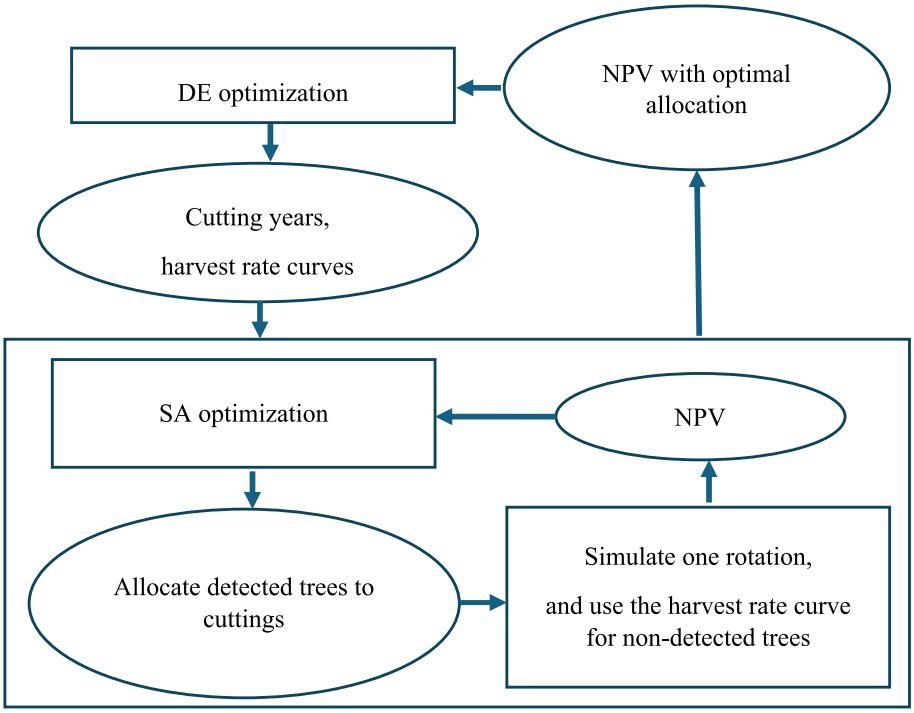

Fig. 3 The layout of the two-level hybrid optimization method. DE stands for differential evolution and SA for simulated annealing

used as well (Bettinger et al. 2002; Fransson et al. 2020). In the same way as in Sun et al. (2022b), differential evolution (DE) was used to find the optimal cutting years. It was assumed that the number of remaining cuttings is decided or known from experience or earlier research.

Optimization was done separately for each of the nine plots (Table 1). As a difference from the method proposed by Sun et al. (2022b), the cutting event was optimized individually only for the detected trees. The number of detected trees per plot ranged from 63 to 216, and the number of non-detected trees ranged from 5 to 96. In the optimization examples of this study, the locations of non-detected were known from the field measurements.

A thinning intensity function was applied to the non-detected trees. The generalized logistic function (Richards 1959) was used:

$$h(d) = \frac{1}{(1 + pQ \times \exp(-pB(d - pM)))^{(1/pQ)}} \quad (1)$$

where, $h(d)$ is the harvest rate at diameter d, and pQ, pB, and pM are parameters optimized for each thinning. Figure 4 shows that the function allows different types of thinning, including thinning from below, thinning from above, or using the same thinning rate in all diameter classes.

The parameters of the thinning intensity function were optimized simultaneously with the cutting years. Therefore, the number of optimized variables was four for each thinning treatment:

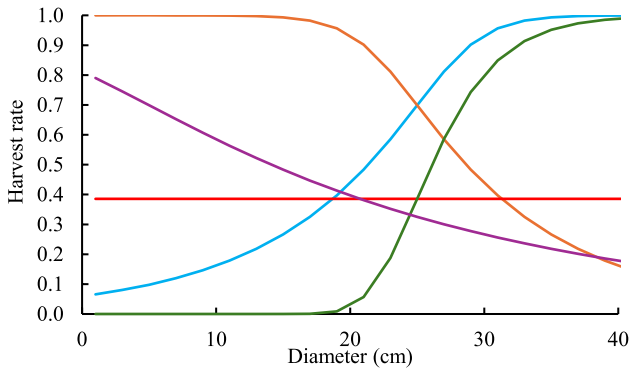

Fig. 4 Examples of thinning intensity functions obtained with different parameter combinations of the generalized logistic function

- Number of years to the thinning (from the beginning or previous cutting).
- Parameters pQ, pB, and pM of the thinning intensity function.

Only one decision variable was required for the final felling: the number of years since the last thinning. For example, if there were three thinning treatments during the rest of the rotation, the number of decision variables was $3 \times 4 + 1 = 13$.

These decision variables were optimized at the higher level of the two-stage method, using DE (Fig. 3). Every candidate solution was passed to a lower-level combinatorial optimization routine, which found the optimal cutting event for each detected tree, provided that the cutting years were

known. Each combination of cutting events that were generated during the SA run was simulated. Simulation means that the stand development and the cuttings were simulated until the final felling. Final felling removed all remaining trees. In thinning treatments, the thinning intensity function was used for trees for which the cutting event was not optimized individually.

The simulation calculated the net present value (NPV) of the management schedule. NPV was first maximized at the lower level, using SA, and keeping the cutting years and thinning intensity functions unchanged. The NPV of the best solution found by SA (best combination of cutting events for trees) was returned to the higher-level DE algorithm, which adjusted the cutting years and the thinning intensity functions.

Optimization algorithms

Differential evolution (DE) was used to optimize the cutting intervals and the thinning intensity functions. It is an optimization algorithm suitable for continuous decision variables (Storn and Price 1997; Pukkala 2009). The method operates with a population of solution vectors. A solution vector is a set of values of the decision variables (in this study, cutting intervals and parameters of thinning intensity functions). The solution vectors are combined and modified to obtain new candidate solutions.

In this study, the elements of the solution vectors were initialized with uniformly distributed random numbers, which ranged from 5 to 30 years for the cutting interval (except for the first cutting for which the range was 0–30 years from the start of the simulation), 0.1 to 20 for pQ, − 1 to 1 for pB, and 5 to 50 for pM. These values were not used as constraints, i.e., the optimization algorithm was allowed to suggest solutions that were outside these ranges.

The NPV, obtained with the optimal allocation of cutting events for detected trees, was calculated for all initial solution vectors. Then, each solution vector was compared to a new candidate solution. The candidate solution was produced by replacing, with a certain probability, its elements with elements drawn from a "noise vector". The noise vector was produced by combining three solution vectors:

$$y_i = x_{Ci} + \lambda\left(x_{Ai} - x_{Bi}\right) \tag{2}$$

where, y_i is element i of the noise vector, x_{Ai}, x_{Bi} and x_{Ci} are the values of the same element in three, randomly selected solution vectors and λ is a parameter. In one, randomly selected solution vector, all elements were replaced by the noise vector value. In the other vectors, each element was replaced by the noise vector value with a probability of 0.5.

The NPV of the candidate solution was calculated by passing it to the lower-level SA routine, which found the optimal cutting event for each detected tree provided that the cutting years and the thinning intensity functions were those indicated by the candidate solution. If the NPV of the candidate solution was better than that of the non-modified solution vector, the candidate replaced the solution vector.

This process of producing new candidate solutions and comparing them with the current solutions was repeated for 30 iterations. The number of solution vectors (population size) was 10. The value of parameter λ in Eq. 2 was 0.5 (Pukkala 2009; Jin et al. 2018).

Simulated annealing (SA) was used to allocate the detected trees to the cutting events. SA operates with one solution vector that in this study consisted of the cutting events of the detected trees. For example, if the number of detected trees was 100 and the optimized management schedule included three thinning treatments and a clear-felling (4 cuttings), the solution vector had 100 elements, and the value of each element was 1, 2, 3 or 4.

The initial solution vector was produced by selecting the cutting event randomly for each tree. The management schedule corresponding to this solution was simulated, taking the cutting years and the thinning intensity functions for non-detected trees from the higher-level DE algorithm. Then, one detected tree was selected randomly, and its cutting event was replaced by another, randomly selected cutting event. This change is called a move. The move was accepted if it improved the NPV of the cutting schedule. Otherwise, the change was accepted with a probability:

$$p = \left[\frac{NPV_{After} - NPV_{Before}}{T}\right] \tag{3}$$

where, NPV_{Before} is the NPV before changing the cutting event of the selected tree, and NPV_{After} is the NPV of the schedule after the change. T is the "temperature" that determines the probability of accepting changes that do not improve the solution. The temperature was reduced gradually during the search. Therefore, the probability of accepting non-improving changes decreased. The search was stopped when the temperature reached a pre-defined "freezing temperature".

In the optimizations of this study, the starting value of the temperature parameter (T in Eq. 3) was calculated as $T = 0.1 \times 100{,}000 \,/\, N_{detected}$ ($N_{detected}$ is the number of detected trees). Pukkala and Heinonen (2006) suggested that the starting temperature should be of the same magnitude as the maximum effect of an SA move on the objective function value. The above formula calculates the approximate maximum effect of changing the cutting event of one tree on the net present value of the cutting schedule. The number of candidate solutions produced at each temperature was

0.7 times the number of detected trees. A new temperature was obtained by multiplying the current temperature by 0.8. The search was terminated once the temperature reached a value of 0.05 times the starting temperature (Pukkala and Heinonen 2006; Jin et al. 2016).

Calculation of net present value

The incomes from cuttings were discounted to the starting year of the simulation. The NPV of future rotations was considered by adding bare land value to the income of the final felling. For this, a new model for bare land value was developed by optimizing the treatment schedules of 53 plots measured in young pre-commercial larch plantations, assuming that the optimal management schedule included three thinning treatments and a clear felling (Peng et al. 2018). In these optimizations, the cutting years and thinning intensity functions were optimized. All costs and incomes were discounted to the planting year, and it was assumed that the same rotation was repeated to infinity. The management costs before the first commercial cutting were: site preparation in Year 0, 2000 RMB ha^{-1} (RMB stands for renminbi, which is the official currency of China); planting in Year 0, 5000 RMB ha^{-1}; tending in Year 10, 700 RMB ha^{-1} (Peng et al. 2018).

Timber assortments and their stumpage prices are shown in Table 3 (Dong et al. 2022). The same assortment definitions and prices were used in all optimizations of this study.

The optimization results were used to fit the following model that calculates the bare land value of a larch plantation as a function of discount rate and site index.

$$NPV_{\mathrm{BareLand}} = \exp(a_0 + a_1 \ln(SI) + a_2 \ln(Rate + 1)) \quad (4)$$

The site index was calculated with the model of Dong et al. (2021). Site index (*SI*) refers to dominant height at 30 years. The distance-independent individual-tree growth and survival models of Dong et al. (2021) were used in the optimizations that were conducted to obtain bare land values. The same models were also used in the two-level hybrid optimizations. Tree height was predicted with the model of Dong. et al. (2021), and assortment volumes of harvested trees were calculated with the taper models of Peng et al. (2018).

Table 3 Definitions and stumpage prices of timber assortments

Assortment	Minimum top diameter (cm)	Minimum log length (m)	Stumpage price (RMB m^{-3})
Large log	29	4	850
Medium-sized log	19	4	650
Small log	13	4	400
Pulpwood	7	2	250
Firewood	2	1	80

Results

Model for bare land value

The model for bare land value was:

$$NPV_{\mathrm{BareLand}} = \exp(9.99565 + 1.55708\ln(SI) - 2.49050\ln(Rate + 1)) \quad (5)$$

The unit of bare land value is RMB/ha and *Rate* is the discount rate in percent. Figure 5 shows the relationship between the discount rate and bare land value and the variation of bare land value within each discount rate. Most of this variation is explained by the site index. The model predicted well the NPVs of the optimized management schedules (Fig. 6).

Effect of detection rate on NPV

To analyze the effect of the detection rate on the optimization result, either the true detection result was used, or it was assumed that none or all trees were detected. This was possible because the plots had been measured in the field. The results showed that the NPV of the optimized schedule improved, on average, by 5.3% if the cutting event was optimized individually for all trees, as compared to the case where removals were based on optimized harvest rate curves (Fig. 7).

Usually, the largest and most valuable trees are detected. These trees have the strongest effect on the NPV. Therefore,

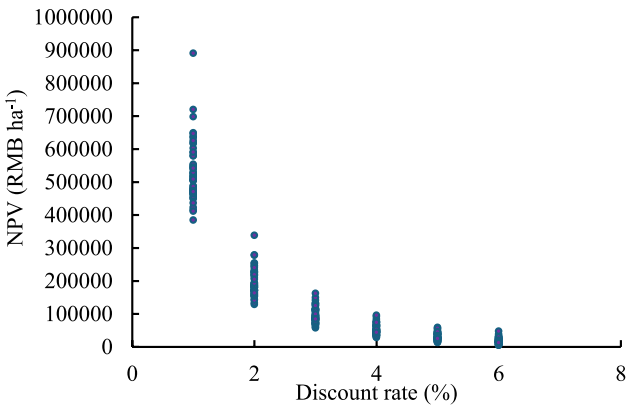

Fig. 5 Net present values are calculated to infinity for the management schedules of 53 plots measured in pre-commercial larch plantations when the management schedule is optimized with different discount rates

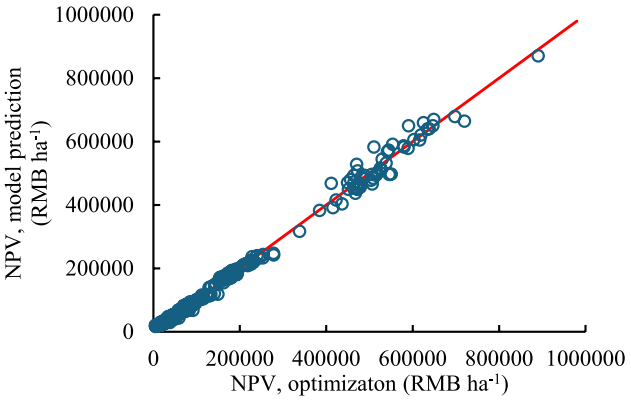

Fig. 6 Correlation between the NPVs of the optimized management schedules and NPVs predicted with the model (Eq. 5)

the improvement in the NPV was only 1.1% when all trees were assumed to be detected, compared to the optimization that was based on the true detection result. The difference between the case where no trees were detected, and the true detection rate was 4.3%. This is also the improvement when the optimization approach is changed from the diameter distribution approach (thinning intensity function used for all trees) to the hybrid approach. The improvement was 3.1% in middle-aged stands and 5.2% in young stands. The benefit of using the hybrid approach was larger for young stands although the detection rate was lower in these stands. The result shows that it is worthwhile to use the hybrid approach whenever individually detected trees are available for management optimization.

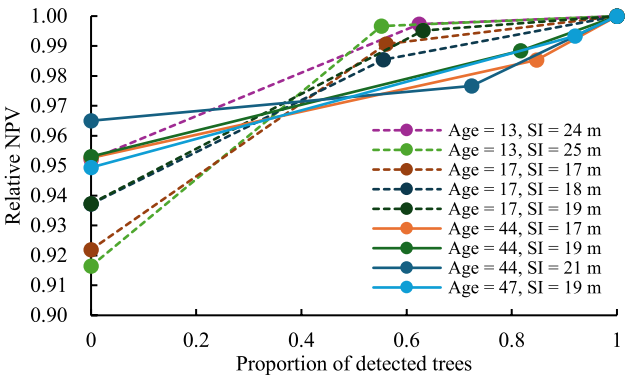

Fig. 7 Relative NPVs of the optimized three-cutting management schedules as a function of the proportion of detected and individually optimized trees. The NPV of the case where the cutting events were optimized individually for all trees gets a value equal to one, and the other NPVs are expressed as the proportion of the maximal NPV. Continuous lines represent 44–47-year-old stands and dotted lines represent 13–17-year-old stands

Detailed results for two plots

One plot measured in a 44-year-old plantation and another plot measured in a 17-year-old plantation were used to visualize the optimal management schedule and inspect the similarity of the optimization results in the three different cases (no trees detected, true detection result used, all trees detected).

In the plot that represents middle-aged plantations (Fig. 8), the first thinning treatment was to be conducted immediately or almost immediately, and the final felling was proposed 9 or 10 years later. The thinning was very heavy in all three cases. The thinning was from above when a part or all trees were assumed to be detected. The thinning treatment reduced the mean diameter from 23.2 to 19.1 cm (true detection rate used) or from 23.2 to 19.3 cm (all trees

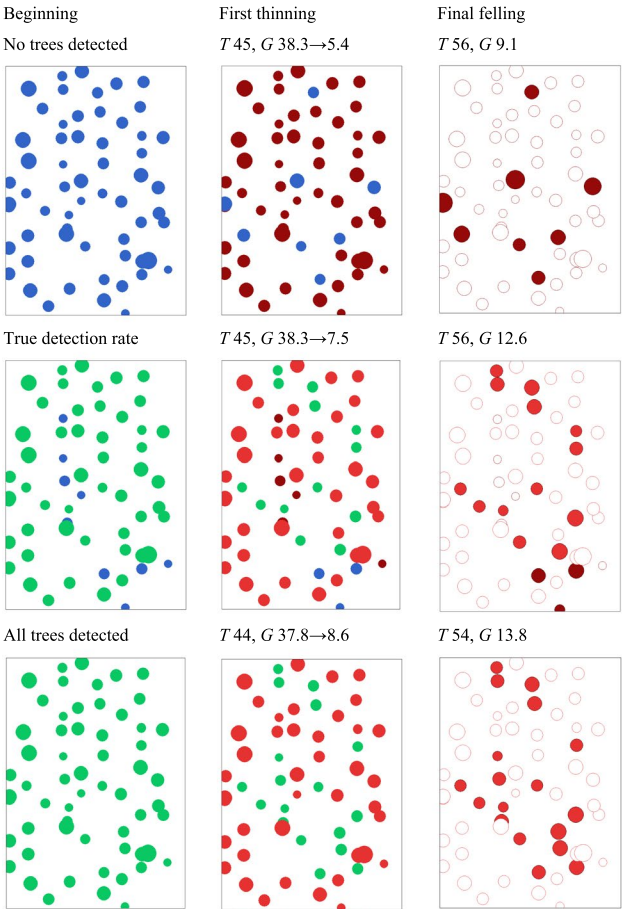

Fig. 8 Tree map of a 20 m by 30 m sample plot measured in a 44-year-old larch plantation. The green color stands for trees that were detected from LiDAR data, and the blue color stands for non-detected trees. Dark red indicates harvested non-detected tree and lighter red indicates harvested detected tree. Open circles are trees that were removed in earlier cuttings. The diameter of the circle is proportional to the DBH of the tree. *T* is stand age (years), *G* is stand basal area (m^2 $ha.^{-1}$)

detected). When no trees were detected, the mean diameter of trees did not change in the thinning treatment.

In the five young stands in which the hybrid method was tested, 4-cutting schedules produced 5.2% higher average NPV than 3-cutting schedules, when the hybrid method was used with the true number of individually detected trees. Therefore, 4-cutting schedules of a young sample plot were visualized and compared with three different assumptions concerning the number of detected trees.

When it was assumed that no trees were detected, the first thinning was at the age of 34 years, and it removed both small and large trees (Fig. 9). The same was true for the second thinning, conducted at the age of 41 years, but the treatment resembled more thinning from above (Fig. 10) as the mean diameter decreased from a pre-thinning value of 15.8 cm to a post-thinning value of 13.5 cm. The third thinning at 67 years removed predominantly large trees. The remaining basal area was very low, only 4.4 m^2 ha^{-1}. The results suggest that it was more profitable to let the smallest trees of the stand grow for another 16 years rather than remove all trees at 67 years.

Optimization based on the true detection result produced a rather similar outcome (Fig. 9, middle). The first thinning removed trees from both ends of the diameter distribution. All non-detected trees were removed in the first thinning. The second and third thinning treatments removed mainly large trees. The third thinning left a low number of small trees to continue growing for 22 years.

The third optimization case, where the cutting event of all trees was optimized individually, produced a cutting schedule that resembled the previous ones (Fig. 9, bottom). The first thinning removed both small and large trees, but the subsequent cuttings represented thinning from above. Again, the third thinning left a low number of the smallest trees to continue growing, in this case for 29 years.

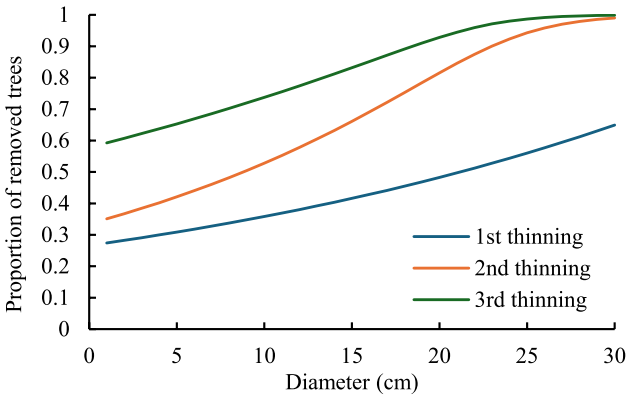

Fig. 10 Optimal thinning intensity functions for the young plot in the optimization where all thinning removals were based on the harvest rate curves (top row in Fig. 9)

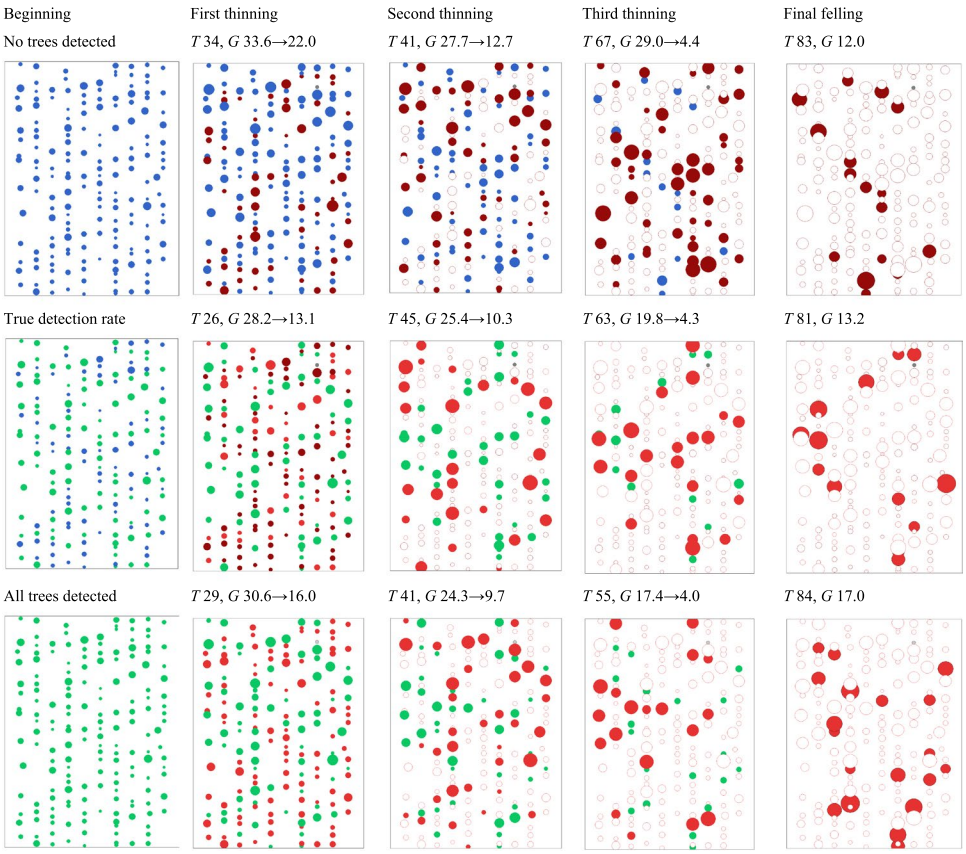

Fig. 9 Optimal thinning ages and tree removals when the optimization was based on the assumption that no trees were detected (top), true detection result was used (middle) or all trees were assumed to be detected (bottom). The blue color is a remaining non-detected tree, the green color is a remaining detected tree, and the red color is a removed tree (dark red is a non-detected tree, and light red is a detected tree). Open circles refer to trees that were removed in earlier cuttings. *T* is stand age (years), *G* is stand basal area (m^2 $ha.^{-1}$)

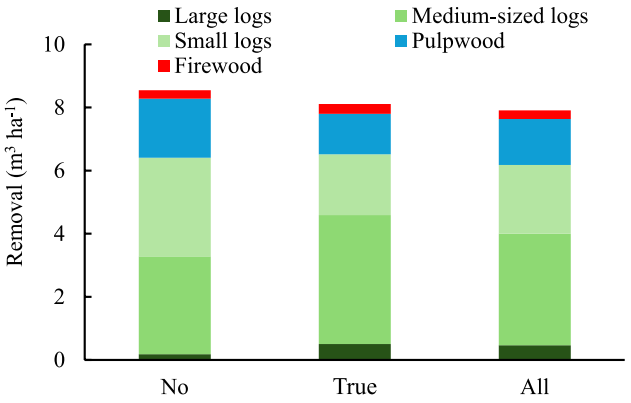

Fig. 11 Mean annual removals calculated over the whole rotation in the optimized four-cutting schedules of a young larch plantation assuming that no trees were detected (No), the true detection result is used (True), or assuming that all trees are detected (All)

The two optimization cases where a part or all trees were detected, and their cutting event was optimized individually, were close to each other also in terms of the assortment distribution of removal (Fig. 11). Most of the removal consisted of medium- and small-sized logs. The production of the most valuable large logs was low in all cases.

Discussion

The motivation behind this study was the increased availability of tree-level data in forest planning. Forest planning methods should adapt to the innovations in the fields of data acquisition and forest inventory. This study suggested a new method for optimizing harvest decisions partly at the individual tree level and partly at the diameter class level. Previous studies on tree-level planning have been conducted for cases where all trees are detected data (Packalen et al. 2020; Pascual 2021; Sun et al. 2022b).

The analyses of this study showed that it is profitable to optimize the cutting event at the tree level whenever tree-level data are available. The largest trees of the stand are the most valuable and financially the most mature for cutting (Pukkala et al. 2015). Often, they are detected better than small trees. Therefore, optimizations, where harvest decisions are optimized individually only for the detected trees, give almost as good results as a optimizing the harvest decision individually for all trees.

It would be technically possible to optimize the harvest decisions of all trees in one step, using available methods for combinatorial optimization problems (e.g., Fransson et al. 2020). This approach could also find the optimal cutting years and result in reasonable harvest volumes if too low or too high annual thinning removals were penalized. However, the decision space of this type of optimization would be enormous (Sun et al. 2022b) resulting in very long computing times. Our method decreased the decision space of the combinatorial tree-level optimization problem by fixing the number of cuttings and optimizing the cutting years at the higher level of a two-step hierarchy of optimization routines. Another way to decrease the decision space was to use tree-level optimization only for the detected trees.

The method suggested in this article is a compromise between reasonable computing time and an attempt to efficiently use the data that modern inventory methods can produce. Together with the bare land model, the system could be used immediately in forestry practice, especially in plantations. However, in forestry practice, the locations of the non-detected trees are unknown. This does not affect optimization if non-spatial growth models are used and there are no spatial forest management objectives. If the simulation of forest development uses distance-dependent models, or a certain spatial distribution of remaining trees is targeted in thinning treatments, the non-detected trees need to be placed in plausible locations. Further research is needed to provide a methodology for generating the locations of non-detected trees.

The suggested hybrid method is flexible in the sense that it is not necessary to use individual tree optimization or the tree-level option can be used only in some stands. Since the distant future involves more uncertainty than the immediate future, and discounting decreases the effect of distant harvest incomes, it is also possible to optimize only the first cutting at the tree level, or perhaps the first and the second cuttings, and use optimized harvest rate curves for all trees in subsequent cuttings.

Even when all or most trees of a stand could be measured or detected individually, it may still be justified to optimize the harvest decision individually for only part of the trees. If the stand consists of upper and lower canopy layers, for example, the cutting moments of the trees in the lower canopy may be so far in the future that it is not worthwhile to extend tree-level optimization to these cutting events. When ingrowth is simulated, it makes sense to use the harvest rule also for the ingrowth trees.

The method described here works also in mixed stands. One of the emerging management objectives of Chinese plantation forests is diversity (Sun et al. 2022b), which may be pursued by planting mixed stands and maintaining the species mixture throughout the rotation. In optimization, the diversity of species mixture can be controlled by including the Shannon index in the objective function (Sun et al. 2022b). Diversity in tree size can be aimed at by using the Gini index as an objective variable (Sun et al. 2022b; Valbuena et al. 2012). The spatial distribution of trees can be regulated by aggregation indices like the Clark and Evans index (Sun et al. 2022b),

or aggregating or dispersing removed trees (Packalen et al. 2020).

The method discussed in this article is not restricted to airborne LiDAR inventories. Individual tree data may be obtained also with other methods such as terrestrial laser scanning (de Paula Pires et al. 2022), ITD from photogrammetric data (Weinstein et al. 2019), visual tree interpretation from digital aerial photographs or even traditional tree measurement in the field. The method that produces information on trees that are not detected individually, can also be other than data imputation based on LiDAR metrics. The diameter distribution can be obtained by predicting the parameters of a distribution function from remote sensing data (Hao et al. 2022), or using histogram matching (Kansanen et al. 2019) and calibration methods (Xu et al. 2014). It is also possible to use field sampling instead of remote sensing methods.

The optimizations of this study were conducted for small sample plots because these plots allowed us to analyze the effect of detection rate on the profitability of optimized management schedules. In forestry practice, however, the calculation unit would be a tree stand or other homogeneous segment of the forest. The decision space of the hybrid method and the solving time of the lower-level combinatorial optimization problem increases exponentially with the increasing number of individually detected trees. This calls for using small stands or segments in management optimization.

The optimizations conducted for the young sample plots often suggested that the first thinning should remove trees from both small and large diameter classes. A similar result that the first thinning should remove trees from both ends of the diameter distribution was obtained earlier by Pukkala et al. (1998) and Hyytiäinen et al. (2005). For small trees, which do not give much income, the reason might be that the trees would die if left to continue growing. The obvious reason for removing large trees is that they give much income and are financially the most mature for cutting (e.g., Pukkala et al. 2015). Later thinning treatments are more and more thinning from above, which is a logical outcome when economic profitability is maximized (Pukkala et al. 2015; Jin et al. 2017; Peng et al. 2018).

Our optimization results should not be taken as guidelines for forestry practice because the management objectives of true decision-makers were not maximized, not even requested. Our optimizations suggested very heavy thinning treatments. Such thinning would increase the risk of wind damage. In addition, the future management of Chinese tree plantations will most probably be multi-objective where the aims might be, in addition to economic profitability, to increase the carbon stocks of forests and produce a more balanced distribution of different timber assortments (Jin et al. 2017; Peng et al. 2018). In the test optimizations of this study, the production of large-sized logs was most probably smaller than what would be regarded acceptable in forestry practice. These considerations call for maintaining higher growing stock densities than obtained in the optimizations and perhaps using longer rotation lengths.

Large-area Forest planning often sets forest-level constraints to guarantee an even flow of timber or control other forest-level management objectives. The method described here optimizes the management of one stand at a time, independently of the other stands. Therefore, the achievement of forest-level management objectives and constraints is not guaranteed. The reduced cost method suggested by Hoganson and Rose (1984) and expanded to spatial problems by Pukkala et al. (2009) could be applied to get the stand-level optimization results to conform to the forest-level constraints. The idea of the reduced-cost method is to penalize the stand-level solutions if the forest-level objectives deviate from their target levels. Dual prices of the forest-level objectives are used as the weights of the deviations. The dual prices are gradually adjusted until the stand-level solutions fulfill the forest-level constraints.

Although the optimizations of this study were conducted for even-aged management, it is also possible to adapt the method to continuous cover forestry (CCF). As shown by Sun et al. (2022b) the harvest decision can be optimized individually also for the ingrowth trees although they are not present in the stand at the start of the simulation. The problem of tree-level optimization in CCF is the high computational burden due to the gradually increasing number of trees during longer-term calculations. Therefore, it is hardly worthwhile to use the tree-level approach for ingrowth trees but apply optimized harvest rate curves for them. Another modification in CCF would be a model for predicting the NPV of the ending forest (e.g., Pukkala 2022), instead of bare land value. This is because, in CCF, the forest is never clear-felled, and bare land value is never required in management optimization. The usual practice is to optimize a certain number of cuttings and predict the NPV of later cuttings with a model (Pukkala 2022).

Conclusion

The study demonstrated the benefit of the suggested two-stage hierarchical method for forest planning in cases where part of the trees is detected or measured individually. Optimizing the cutting event individually for each detected tree improves the profitability of forest management compared to optimizing the dependence of thinning intensity on tree diameter. The hybrid method developed in this study is immediately applicable to forestry practice. The method is suitable for even-aged forest management.

Funding Open access funding provided by University of Eastern Finland (including Kuopio University Hospital).

Declarations

Conflict of interests The authors declare that they have no known competing financial interests or personal relationships that could have appeared to influence the work reported in this paper.

Open Access This article is licensed under a Creative Commons Attribution 4.0 International License, which permits use, sharing, adaptation, distribution and reproduction in any medium or format, as long as you give appropriate credit to the original author(s) and the source, provide a link to the Creative Commons licence, and indicate if changes were made. The images or other third party material in this article are included in the article's Creative Commons licence, unless indicated otherwise in a credit line to the material. If material is not included in the article's Creative Commons licence and your intended use is not permitted by statutory regulation or exceeds the permitted use, you will need to obtain permission directly from the copyright holder. To view a copy of this licence, visit http://creativecommons.org/licenses/by/4.0/.

References

Baskent EZ (2020) A framework for characterizing and regulating ecosystem services in a management planning context. Forests. https://doi.org/10.3390/f11010102

Bettinger P, Graetz D, Boston K et al (2002) Eight heuristic planning techniques applied to three increasingly difficult wildlife planning problems. Silva Fennica 36:561–584. https://doi.org/10.14214/sf.545

Brede B, Calders K, Lau A et al (2019) Non-destructive tree volume estimation through quantitative structure modelling: comparing UAV laser scanning with terrestrial LIDAR. Remote Sens Environ 233:111355. https://doi.org/10.1016/j.rse.2019.111355

Chen Q, Baldocchi D, Gong P, Kelly M (2006) Isolating individual trees in a savanna woodland using small footprint LIDAR data. Photogramm Eng Remote Sens 72:923–932. https://doi.org/10.14358/PERS.72.8.923

Contreras MA, Chung W (2013) Developing a computerized approach for optimizing individual tree removal to efficiently reduce crown fire potential. For Ecol Manag 289:219–233. https://doi.org/10.1016/j.foreco.2012.09.038

de Paula PR, Olofsson K, Persson HJ et al (2022) Individual tree detection and estimation of stem attributes with mobile laser scanning along boreal forest roads. ISPRS J Photogrammetry Remote Sens 187:211–224. https://doi.org/10.1016/j.isprsjprs.2022.03.004

Dong L, Pukkala T, Li F, Jin X (2021) Developing distance-dependent growth models from irregularly measured sample plot data—a case for Larix olgensis in Northeast China. For Ecol Manage 486:118965. https://doi.org/10.1016/j.foreco.2021.118965

Dong L, Bettinger P, Qin H, Liu Z (2022) Optimizing rotation lengths for maximizing carbon balance of larch plantations in northeast China. J Clean Prod 343:131025. https://doi.org/10.1016/j.jclepro.2022.131025

Fransson P, Franklin O, Lindroos O et al (2020) A simulation-based approach to a near-optimal thinning strategy: allowing harvesting times to be determined for individual trees. Can J for Res 50:320–331. https://doi.org/10.1139/cjfr-2019-0053

Gobakken T, Næsset E (2004) Estimation of diameter and basal area distributions in coniferous forest by means of airborne laser scanner data. Scand J for Res 19:529–542. https://doi.org/10.1080/02827580410019454

Hao Y, Widagdo FRA, Liu X et al (2021) Individual tree diameter estimation in small-scale forest inventory using UAV laser scanning. Remote Sens. https://doi.org/10.3390/rs13010024

Hao Y, Widagdo FRA, Liu X et al (2022) Estimation and calibration of stem diameter distribution using UAV laser scanning data: a case study for larch (*Larix olgensis*) forests in Northeast China. Remote Sens Environ 268:112769. https://doi.org/10.1016/j.rse.2021.112769

Hoganson HM, Rose DW (1984) A simulation approach for optimal timber management scheduling. For Sci 30(1):220–238. https://doi.org/10.1093/forestscience/30.1.220

Hyytiäinen K, Tahvonen O, Valsta L (2005) Optimum juvenile density, harvesting, and stand structure in even-aged Scots pine stands. For Sci 51(2):120–133. https://doi.org/10.1093/forestscience/51.2.120

Jeronimo SMA, Kane VR, Churchill DJ et al (2018) Applying LiDAR individual tree detection to management of structurally diverse forest landscapes. J for 116:336–346. https://doi.org/10.1093/jofore/fvy023

Jin X, Pukkala T, Li F (2016) Fine-tuning heuristic methods for combinatorial optimization in forest planning. Eur J for Res 135:765–779. https://doi.org/10.1007/s10342-016-0971-x

Jin XJ, Pukkala T, Li FR, Dong LH (2017) Optimal management of Korean pine plantations in multifunctional forestry. J for Res 28(5):1027–1037. https://doi.org/10.1007/s11676-017-0397-4

Jin X, Pukkala T, Li F (2018) Meta optimization of stand management with population-based methods. Can J for Res 48:697–708. https://doi.org/10.1139/cjfr-2017-0404

Kansanen K, Vauhkonen J, Lähivaara T et al (2019) Estimating forest stand density and structure using Bayesian individual tree detection, stochastic geometry, and distribution matching. ISPRS J Photogrammetry Remote Sen 152:66–78. https://doi.org/10.1016/j.isprsjprs.2019.04.007

Kappen G, Kastner E, Kurth T, Puetz J, Reinhardt A, Soininen J (2020) The staggering value of forests-and how to save them. In: Boston consulting group. https://www.bcg.com/publications/2020/the-staggering-value-of-forests-and-how-to-save-them

Leite RV, Silva CA, Mohan M et al (2020) Individual tree attribute estimation and uniformity assessment in fast-growing *Eucalyptus* spp. Forest Plantations Using Lidar Linear Mixed-Effects Models Remote Sens. https://doi.org/10.3390/rs12213599

Liu K, Shen X, Cao L et al (2018) Estimating forest structural attributes using UAV-LiDAR data in Ginkgo plantations. ISPRS J Photogramm Remote Sens 146:465–482. https://doi.org/10.1016/j.isprsjprs.2018.11.001

Maltamo M, Malinen J, Packalén P et al (2006) Nonparametric estimation of stem volume using airborne laser scanning, aerial photography, and stand-register data. Can J for Res 36:426–436. https://doi.org/10.1139/x05-246

Mohan M, Silva CA, Klauberg C et al (2017) Individual tree detection from unmanned aerial vehicle (UAV) derived canopy height model in an open canopy mixed conifer forest. Forests. https://doi.org/10.3390/f8090340

Næsset E (2002) Predicting forest stand characteristics with airborne scanning laser using a practical two-stage procedure and field data. Remote Sens Environ 80:88–99. https://doi.org/10.1016/S0034-4257(01)00290-5

Packalén P, Maltamo M (2008) Estimation of species-specific diameter distributions using airborne laser scanning and aerial photographs. Can J for Res 38:1750–1760. https://doi.org/10.1139/X08-037

Packalén P, Temesgen H, Maltamo M (2012) Variable selection strategies for nearest neighbor imputation methods used in remote sensing based forest inventory. Can J Remote Sens 38:557–569. https://doi.org/10.5589/m12-046

Packalen P, Strunk JL, Pitkänen JA et al (2015) Edge-tree correction for predicting forest inventory attributes using area-based approach with airborne laser scanning. IEEE J Sel Top Appl Earth Obs Remote Sens 8:1274–1280. https://doi.org/10.1109/JSTARS.2015.2402693

Packalen P, Pukkala T, Pascual A (2020) Combining spatial and economic criteria in tree-level harvest planning. For Ecosyst. https://doi.org/10.1186/s40663-020-00234-3

Pan Y, Birdsey RA, Fang J et al (1979) (2011) A large and persistent carbon sink in the world's forests. Science 333:988–993. https://doi.org/10.1126/science.1201609

Pascual A (2021) Multi-objective forest planning at tree-level combining mixed integer programming and airborne laser scanning. For Ecol Manage 483:118714. https://doi.org/10.1016/j.foreco.2020.118714

Pascual A, Guerra-Hernández J (2022) Spatial connectivity in tree-level decision-support models using mathematical optimization and individual tree mapping. For Policy Econ 139:102732. https://doi.org/10.1016/j.forpol.2022.102732

Pascual A (2019) Using Tree Detection Based on Airborne Laser Scanning to Improve Forest Inventory Considering Edge Effects and the Co-Registration Factor. Remote Sens 11:. https://doi.org/10.3390/rs11222675

Peng W, Pukkala T, Jin X, Li F (2018) Optimal management of larch (Larix olgensis A. Henry) plantations in Northeast China when timber production and carbon stock are considered. Ann for Sci 75:63. https://doi.org/10.1007/s13595-018-0739-1

Peuhkurinen J, Mehtätalo L, Maltamo M (2011) Comparing individual tree detection and the area-based statistical approach for the retrieval of forest stand characteristics using airborne laser scanning in Scots pine stands. Can J for Res 41:583–598. https://doi.org/10.1139/X10-223

Pippuri I, Maltamo M, Packalen P, Mäkitalo J (2013) Predicting species-specific basal areas in urban forests using airborne laser scanning and existing stand register data. Eur J for Res 132:999–1012. https://doi.org/10.1007/s10342-013-0736-8

Pukkala T (2009) Population-based methods in the optimization of stand management. Silva Fennica 43:261–274. https://doi.org/10.14214/sf.211

Pukkala T (2022) Improved guidelines for any-aged forestry. J for Res 33(5):1443–1457. https://doi.org/10.1007/s11676-022-01473-6

Pukkala T, Heinonen T (2006) Optimizing heuristic search in forest planning. Nonlinear Anal Real World Appl 7:1284–1297. https://doi.org/10.1016/j.nonrwa.2005.11.011

Pukkala T, Miina J, Kurttila M, Kolström T (1998) A spatial yield model for optimizing the thinning regime of mixed stands of Pinus sylvestris and Picea abies. Scand J for Res 13:31–42. https://doi.org/10.1080/02827589809382959

Pukkala T, Heinonen T, Kurttila M (2009) An application of a reduced cost approach to spatial forest planning. For Sci 55(1):13–22. https://doi.org/10.1093/forestscience/55.1.13

Pukkala T, Lähde E, Laiho O (2015) Which trees should be removed in thinning treatments? For Ecosyst 2:32. https://doi.org/10.1186/s40663-015-0056-1

Quan Y, Li M, Hao Y, Wang B (2021) Comparison and evaluation of different pit-filling methods for generating high resolution canopy height model using UAV laser scanning data. Remote Sens. https://doi.org/10.3390/rs13122239

Richards F (1959) A flexible growth function for empirical use. J Exp Bot 10:290–300. https://doi.org/10.1093/jxb/10.2.290

Storn R, Price K (1997) Differential evolution—a simple and efficient heuristic for global optimization over continuous spaces. J Global Optim 11:341–359. https://doi.org/10.1023/A:1008202821328

Sun Y, Wang W, Pukkala T, Jin X (2021) Stand delineation based on laser scanning data and simulated annealing. Eur J for Res 140:1065–1080. https://doi.org/10.1007/s10342-021-01384-x

Sun Y, Jin X, Pukkala T, Li F (2022a) Predicting individual tree diameter of larch (Larix olgensis) from UAV-LiDAR data using six different algorithms. Remote Sens. https://doi.org/10.3390/rs14051125

Sun Y, Jin X, Pukkala T, Li F (2022b) Two-level optimization approach to tree-level forest planning. For Ecosyst 9:100001. https://doi.org/10.1016/j.fecs.2022.100001

Sun Y, Jin X, Pukkala T, Li F (2022c) A comparison of four methods for automatic delineation of tree stands from grids of LiDAR metrics. Remote Sens. https://doi.org/10.3390/rs14246192

Valbuena R, Packalen P, Martı´n-Fernández S, Maltamo M (2012) Diversity and equitability ordering profiles applied to study forest structure. For Ecol Manage 276:185–195. https://doi.org/10.1016/j.foreco.2012.03.036

Vauhkonen J, Ene L, Gupta S et al (2012) Comparative testing of single-tree detection algorithms under different types of forest. Forestry Int J Forest Res 85:27–40. https://doi.org/10.1093/forestry/cpr051

Wang M, Im J, Zhao Y, Zhen Z (2022) Multi-platform LiDAR for Non-destructive individual aboveground biomass estimation for Changbai Larch (Larix olgensis Henry) using a Hierarchical Bayesian approach. Remote Sens. https://doi.org/10.3390/rs14174361

Weinstein BG, Marconi S, Bohlman S et al (2019) Individual Tree-Crown Detection in RGB Imagery Using Semi-Supervised Deep Learning Neural Networks. Remote Sens. https://doi.org/10.3390/rs11111309

Wing BM, Boston K, Ritchie MW (2019) A technique for implementing group selection treatments with multiple objectives using an airborne Lidar-derived stem map in a heuristic environment. Forest Sci 65:211–222. https://doi.org/10.1093/forsci/fxy050

Xiao W, Xu S, Elberink SO, Vosselman G (2016) Individual tree crown modeling and change detection from Airborne Lidar data. IEEE J Sel Top Appl Earth Obs Remote Sens 9:3467–3477. https://doi.org/10.1109/JSTARS.2016.2541780

Xu Q, Hou Z, Maltamo M, Tokola T (2014) Retrieving suppressed trees from model-based height distribution by combining high- and low-density airborne laser scanning data. Can J Remote Sens 40:233–242. https://doi.org/10.1080/07038992.2014.935933

Yu X, Hyyppä J, Holopainen M, Vastaranta M (2010) Comparison of area-based and individual tree-based methods for predicting plot-level forest attributes. Remote Sens 2:1481–1495. https://doi.org/10.3390/rs2061481

Zaforemska A, Xiao W, Gaulton R (2019) Individual tree detection from UAV Lidar data in a mixed species Woodland. In: The international archives of the photogrammetry, remote sensing and spatial information sciences XLII-2/W13: 657–663. https://doi.org/10.5194/isprs-archives-XLII-2-W13-657-2019

Publisher's Note Springer Nature remains neutral with regard to jurisdictional claims in published maps and institutional affiliations.